Resour Environ Inf Eng, 2022, 4(1): 200-212
DOI: 10.25082/REIE.2022.01.004

RESEARCH ARTICLE

Experimental investigation of gamma Stirling engine coupling to convert thermal to cooling energy in different laboratory conditions

Hamidreza Asemi[1] **Sareh Daneshgar**[2] **Rahim Zahedi**[3*]

[1] Faculty of Engineering, Science and Research Branch, Islamic Azad University, Tehran, Iran
[2] Faculty of Electrical Engineering, Iran University of Science and Technology, Tehran, Iran
[3] Department of Renewable energy and Environmental Engineering, University of Tehran, Tehran, Iran

Correspondence to: Rahim Zahedi, Department of Renewable energy and Environmental Engineering, University of Tehran, Tehran, Iran;
Email: rahimzahedi@ut.ac.ir

Received: September 22, 2022;
Accepted: October 31, 2022;
Published: November 3, 2022.

Citation: Asemi H, Daneshgar S and Zahedi R. Experimental investigation of gamma Stirling engine coupling to convert thermal to cooling energy in different laboratory conditions. *Resour Environ Inf Eng*, 2022, **4**(1): 200-212. https://doi.org/10.25082/REIE.2022.01.004

Abstract: The main aim of this research is to experimentally investigate the two coupled identical ST500 gamma-type Stirling engines and convert thermal energy to cooling energy. Using a new structure and two coupled Stirling engines at different temperatures and pressures and use of biomass fuel within the 4 -8 bar average pressure range of the first engine heat source, the 1-4 bar average pressure range of the second engine heat sink, and Stirling heat engine temperature range of 480-580°C, the effective cooling is obtained in the cooling engine. In doing tests, attempts were made to reach lower than 9 percent error results in different parts of engine, including insulation, fluid leakage, belt loosing, and measurement devices. According to the obtained results, 8 bars increase in the average pressure range of the gas in the first engine heat source, a 1 bar reduction in the average pressure range of the gas in the second engine heat sink, the increased temperature of the heat source up to 580°C, and the use of the light operating fluid such as helium will affect the generation of cooling up to -16°C.

Keywords: cooling, power supply, gamma Stirling, biomass

1 Introduction

Stirling motor is one of the types of heat air motors that, like other types of heat motors, can produce mechanical or electrical work by using heat exchange between heat and heat sinks [1]. Heat enters the engine at a warm temperature, part of it is converted to mechanical or electrical work, and the rest leaves the engine at a cooler temperature. The Stirling engine is simple in performance and has good torque, and if used in reverse can be a good alternative to refrigeration cycles [2]. Today, the introduction of new correlations and sealing materials, as well as the use of advanced software and computers that facilitate accurate and complex calculations, will accelerate the evolution of this engine. If it is not possible to optimize existing engines to reduce the amount of fuel and emissions and noise to the international standards of environmental organizations, Stirling engines should definitely be considered [3].

1.1 Types of Stirling engines

Stirling engines have been developed over the years and various designs of this type of engine have been developed [4]. Different types of motor Stirling are known as alpha, beta, gamma and free semolina. The principles of thermodynamics are the same for all of them, and their main difference is in the way the different components of the engine are placed next to each other. All Stirling engines have five inhibitory volumes, which are compression chamber, coolant, recovery, heating and expansion chamber, respectively.

1.1.1 Alpha type engine

Alpha engines have two separate cylinders for compression and expansion spaces and one cylinder in each cylinder. The two separate cylinders are connected by a heat sink and a connecting pipe. The heat cylinder is placed next to the heat source and the cooling cylinder is placed next to the heat sink. These types of engines, conceptually, have the simplest configuration among all types of Stirling engines. However, the need to seal both cylinders is one of its disadvantages and the problem of heat cylinder sealing due to contact with the heat source is one of its technical problems [5]. Figure 1 shows the schematic of the alpha-type Stirling engine.

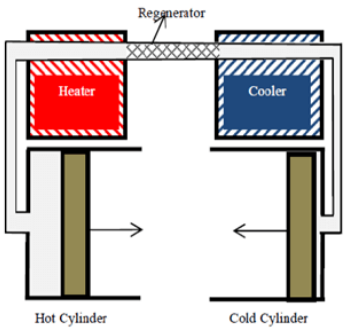

Figure 1 Schema Alpha Type Stirling engine

1.1.2 Beta type engine

Figure 2 shows the beta type Stirling engine, the oldest building of Stirling engines. Robert Stirling's invention as the first Stirling engine had a beta structure. Beta engines use a configuration of power pump and displacement. The structure of the motor is such that both cylinders are placed in a cylinder linearly [6].

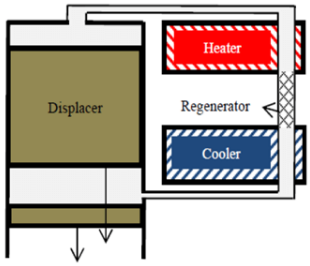

Figure 2 Schema Beta Type Stirling engine

1.1.3 Gamma type engine

The gamma-type Stirling engine, like the beta-type engine, has a moving pump configuration. In this type of motor, the pump and the displacement are in two separate cylinders. The Gamma Stirling Engine has a lower compression ratio than the Alpha and Beta models, but because only the power pump needs and it is sealed and the cylinders are separate [7]. It has the simplest mechanical arrangement among other types of Stirling engines [8]. Figure 3 shows the scheme of the gamma-type Stirling engine.

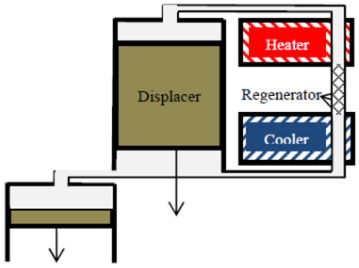

Figure 3 Schema Gamma Type Stirling engine

1.2 Background

Jahani Kaldehi et al. [9]. designed a Stirling engine to generate electricity, heating and cooling at the same time in a residential area with a different climate. The engine is alpha and the system is simulated in GT Suite software. According to the results, the maximum efficiency is between 79 to 88% in different climatic conditions and the designed system leads to a reduction of air pollution by reducing CO, CO2 and NOX and the leakage of this system at low pressures showed a lower value. Prakash [10] have investigated the effect of increasing efficiency due to the use of Stirling motor in the combined cycle of ironing and Stirling. The Stirling engine provides the required electrical load to the vehicle under test using a temperature difference of 75°C between heat and heat sinks. In this design, the Stirling engine rotates the car's power generator instead of the engine belt. In their research, Hushang et al. [11, 12] improved the gas transfer motors in the solar Stirling engine to increase efficiency and also improved the gas displacement variables including the amplitude, state and frequency of the Stirling motor so that the heat efficiency and production capacity The engine increases.

In order to ensure the calculations of the mathematical model, an experiment was designed and performed on a gamma-type Stirling engine using a third-order thermodynamic analysis program, during which the absolute fluid pressure, crankshaft angle and velocity were read and recorded instantly [13]. Also, the generating power of the engine was measured using a generator and the results of the mathematical model were compared with the measured values under the same test conditions and its performance was ensured and the average error of the mathematical and experimental simulations was about 10%. Dai et al. [14] analyzed the Stirling engine process using limited time thermodynamics and the hypothesis of uniform temperature distribution and investigated the effect of different variables and its limitations. Zia Bashar Hagh and Mahmoodi [15] conducted studies on beta-type Stirling engines and based on the obtained results showed that by changing the operating gas and using Helium gas instead of air gas, the amount of heat output and engine output power decreases while engine efficiency increases. Helium will be a good option if the heat input to the engine is high. Another result of this research is that the energy flow in the Stirling engine recovery is calculated to be approximately 5 times higher than that of the heater and 6 times higher than that of the coolant. Also, as the stroke diameter of the Stirling engine increases, the power decreases while the efficiency of the Stirling engine increases.

L. Berrin et al. [16] examined the overall performance of the refrigerator for the Stirling pair heat engine and the amount of work related to the final cooling with respect to structural effects and variables such as the temperature ratio for the engine and its density. Ansari Nasab et al. [17] Studied the configuration of a Stirling engine with a molten carbonate fuel cell, a gas turbine to generate electricity, heating and cooling at the same time, and the fundamental and influential variables on the system economically exergy as well as on system costs - through Sensitivity analysis has been reviewed and finally three strategies have been proposed to eliminate unnecessary costs that have improved the performance of the system. Damirchi et al. [18] used a gamma-type Stirling engine to generate heat and electricity simultaneously on a small scale, and at pressures of less than 1 MPa the engine output power was compared experimentally by Schmidt analysis.

Turkyilmazoglu et al. [19] presented thermal response analysis of solid flammable targets at motion. In his research the ignition time and heat flux are predicted regarding the given Peclet numbers. It was concluded that a solid flammable material at motion possesses less ignition time. In another study [20] the coupled energy equations governing the thermal phenomenon of particulate solids and cooling fluid present inside moving bed heat exchangers constructed via a parallel plate system is solved analytically. Results demonstrate how an effective cooling can be achieved with a heat sink mounted on industrial moving bed heat exchangers.

Katooli et al. [21] simulated and experimentally evaluated a Stirling refrigerator unit to convert mechanical electrical energy into energy-cooling energy, and the effects of fluid pressure and generating power for cooling were investigated. Amarloo et al. [22] performed thermodynamic analysis of the functional variables of the new three-cylinder structure of the Stirling engine and its simulation in GT Suite industrial analysis software. The results of the analysis showed that increasing the rotational speed is not suitable for increasing engine performance and has reduced engine efficiency.

Modeling of gamma Stirling-based micro-CCHP systems using different gases as alternative fuels is required to study the influence of the cooling and heat temperatures on the system performance. Thus, an experimental analysis of Gamma Stirling engine that is in accordance with the intrinsic physical principles is essential. In this research, the conversion of electrical energy and mechanical energy for cooling has been done experimentally using a Gamma ST500 type Stirling refrigerator and air and helium operating fluids at different powers and pressures. By increasing the input power of the motor, by changing the voltage, the current of the power supply and the supply pressure of the operating fluid of the Stirling motor, a sub-zero degree of Celsius is achieved. According to the researches, the above method is new and has not been done yet, and more accurate results have been obtained with less error and more accuracy.

2 Methodology

2.1 Accuracy, set up and validation method

The ST500 engine has been used by authors for validation. This program has been tested and validated in the past and its results have been published in authoritative articles [10, 11]. The Nlog program is written by MATLAB and is used for thermodynamic analysis of the Stirling engine. This program is a Stirling engine cycle analysis program that uses quadratic equations. This program calculates the heat output and output power of the Stirling engine. The number of errors in different parts of the engine such as insulation, fluid leakage, belt looseness and engine measuring devices has reached about 10% so that the output results are as accurate as possible.

2.1.1 Engine variables in the program – Nlog

(1) Geometric characteristics of all gas transmission channels, pipes and expansion and compression chambers;
(2) Geometry of connections between moving parts of the engine;
(3) Initial engine pressure and initial temperatures anywhere;
(4) Heat exchanger wall temperature (considered constant over time).

The Nlog code divides all channels of gas transmission tubes in the engine into volume of inhibitions and determines the dynamic and thermodynamic variables for each volume of inhibition by solving the equations of continuity, momentum, and energy. At the beginning and before performing various experiments, an attempt has been made to minimize the amount of errors in different sections and the output results have been studied as carefully as possible.

2.1.2 Sources of error

(1) Insulation of the cooling motor;
(2) Power transmission belt is not strong;
(3) Heat dissipation from water transfer pipes and their insulation;
(4) Leakage of operating fluid in the Stirling refrigerator;
(5) Measuring devices errors.

Considering the power generation period and the Stirling engine flywheel and calculating the belt transmission ratio and the difference between periods, the belt error percentage is less than 10% and therefore it can be said that the existing belt has good power transmission.

2.2 Operating fluid

In general, the best operating fluid is a fluid that, in addition to having physical transfer properties, has a strong heat transfer interval with a low drop due to aerodynamic traction. To achieve such a working fluid, the working fluid must have at least the following characteristics:
(1) Strong conductivity heat transfer coefficient;
(2) strong specific heat capacity;
(3) weak viscosity;
(4) Weak density;
(5) Strong heat transfer capability.

2.3 Mathematical modelling

In this paper, a dynamic, thermodynamic model that has been written and validated for the heating state of the Stirling engine in the past has been used [10]. One of the advantages of using a Stirling engine is the ability to reverse the work cycle. Therefore, it can be used to generate cooling by changing the program pattern. Also, for the validation of the cooling program, optimization and production of cooling in the laboratory using the ST500 gamma type Stirling refrigerator, which was done for the first time in Iran Khodro Research and Development Center (Ipco), the results have been analyzed and studied. The kinematic variables of the engine in question are shown in Figure 4. Gamma type has been proposed for cooling application in various industries, including automobile manufacturing.

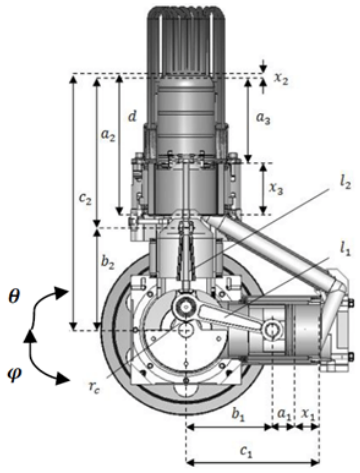

Figure 4 Kinematic variables ST500

The variables φ, rc, l2, l1, d, c2, c1 and a1 to a3 are the structural variables of the engine and have a constant value. Equations (1) and (2) relate these variables to b1 and b2 (the vertical

distance of the semicircle axis at any time up to the crankshaft direction) [23].

$$l_1^2 = r_c^2 + b_1^2 + 2r_c b_1 \cos(\theta) \tag{1}$$

$$l_2^2 = r_c^2 + b_2^2 + 2r_c b_1 \cos(\theta + \varphi) \tag{2}$$

By solving the previous equations for b1 and b2, they are expressed as functions of the crank angle shown in Equations (3) and (4).

$$b_1 = \left(r_c^2 \cos^2\theta + l_1^2 - r_c^2\right)^{1/2} - r_c \cos\theta \tag{3}$$

$$b_2 = \left[\frac{r_c^2 \cos(2\varphi + 2\theta)}{2} + l_2^2 - \frac{r_c^2}{2}\right]^{\frac{1}{2}} - r_c \cos(\varphi + \theta) \tag{4}$$

Thus x1 (compression chamber length), x2 (heat chamber length) and x3 (cooling chamber length) are obtained in terms of the crankshaft angle shown in Equations (5) to (7).

$$x_1 = c_1 - a_1 - b_1 \tag{5}$$

$$x_2 = c_2 - a_2 - b_2 \tag{6}$$

$$x_3 = d - a_3 - x_2 \tag{7}$$

Derivatives x1 and x2 with respect to the crankshaft angle are also shown in Equations (8) and (9). These equations will be used in the section on calculating dynamic equations.

$$\frac{dx_1}{d\theta} = \frac{r_c^2 \sin(2\theta)}{2\left(l_1^2 - r_c^2 \sin^2\theta\right)^{\frac{1}{2}}} = r_c \sin(\theta) \tag{8}$$

$$\frac{dx_2}{d\theta} = \frac{r_C^2 \sin(2\varphi + 2\theta)}{2\left(\frac{r_C^2 \cos(2\varphi+2\theta)}{2} + l_2^2 - r_C^2 - \frac{r_C^2}{2}\right)^{\frac{1}{2}}} - r_c \sin(\varphi + \theta) \tag{9}$$

The first time derivatives x_1 and x_2, which represent the velocity of the moving parts of the engine using equations (10) and (11), and their second derivatives, which represents their acceleration from equations (12) and (13) according to the rules of chain derivative Are calculated.

$$\dot{X}_1 = \frac{dx_1}{dt} = \dot{\theta}\frac{dx_1}{d\theta} \tag{10}$$

$$\dot{X}_2 = \frac{dx_2}{dt} = \dot{\theta}\frac{dx_2}{d\theta} \tag{11}$$

$$\ddot{x}_1 = \frac{d^2x_1}{dt^2} = \dot{\theta}\frac{d\dot{x}_1}{d\theta} \tag{12}$$

$$\ddot{x}_2 = \frac{d^2x_2}{dt^2} = \dot{\theta}\frac{d\dot{x}_2}{d\theta} \tag{13}$$

2.3.1 Kinetic equations of the model

In this section, we seek to find a differential equation that solves the momentum and angular momentum of the crankshaft, and for this purpose, the Lagrange dynamic method is used. The general form of Lagrange equations is shown in Equations 14-17. The sum of the kinetic energies of all the moving parts of the engine will be in the variable T_θ and the sum of the potential energies of the components will be in the variable V_θ. Lagrange in is obtained by the difference of the total kinetic energy from the total potential energy, and finally by placing Lagrange in in the principal Lagrange in equation (equation 17) and performing the necessary derivations, the dynamic differential equation of the Stirling engine is obtained. The torque is equivalent to the engine crankshaft while indicating the crankshaft angle [24].

$$T_\theta = \sum_{i=n_2} \frac{1}{2} m_i \dot{x_i}^2 + \sum_{i=n_r} \frac{1}{2} J_i \dot{\theta_i}^2 \tag{14}$$

$$v_\theta = \sum_{i=n_s} \frac{1}{2} k_i x_i^2 \tag{15}$$

$$T_\theta = T_\theta - v_\theta = \frac{1}{2}\left(\sum_{i=n_1} m_i \dot{x_i}^2 + \sum_{i=n_r} J_i \dot{\theta_i}^2 - \sum_{i=n_s} k_i x_i^2\right. \tag{16}$$

$$\frac{d}{dt}\left(\frac{\partial l_e}{\partial \dot{\theta}}\right) - \frac{\partial l_e}{\partial \theta} = I_c \tag{17}$$

According to the number of variables considered, Lagrange in is obtained as an equation (18).

$$L_e = \frac{1}{2}m_1\dot{x_1^2} + \frac{1}{2}m_2\dot{x_2^2} + \frac{1}{2}J_c\dot{\theta^2} \tag{18}$$

By substituting equations (10) and (11) in Equation (18), finally equation (19) is obtained.

$$L_\theta = \frac{1}{2}\dot{\theta}\left[m_1\left(\frac{dx_1}{d\theta}\right)^2 + m_2\left(\frac{dx_2}{d\theta}\right)^2 + J_c\right] \tag{19}$$

The derivatives calculated in Equations (8) and (9) (in Equation 19) are placed and Lagrange in is obtained in terms of crankshaft angle and crankshaft angle velocity according to Equation (20).

$$L_\theta = \frac{1}{2}\dot{\theta}\{m_1\left[\frac{r_c^2 sin2\theta}{\sqrt[2]{l_1^2 - r_c^2 sin^2\theta}} - r_c sin\theta\right]^2 + m_2\left[\frac{r_c^2 sin(2\varphi+2\theta)}{\sqrt[2]{\frac{r_c^2 sin(2\varphi+2\theta)}{2} + l_2^2\frac{r_c^2}{2}}} - r_c sin(\varphi+\theta\right]^2 + 1\} \tag{20}$$

Therefore, if the derivatives of the Lagrange equation are applied to the Lagrangin, one unit is added to the degree of the derivative in the equations and the left part of the Lagrange equation becomes a function of the angle, velocity and acceleration of the crankshaft to the form of equation (21) [25].

$$\frac{d}{dt}(\frac{\partial L_\theta}{\partial\dot{\theta}} = f(\ddot{\theta}, \theta, \dot{\theta}) \tag{21}$$

3 The Stirling engine used in this research

In this research, the optimization process has been performed on the Stirling ST500 gamma type engine manufactured by Ipco in Figure 5 to produce cooling. The technical specifications of this engine are also listed in Table 1 [10].

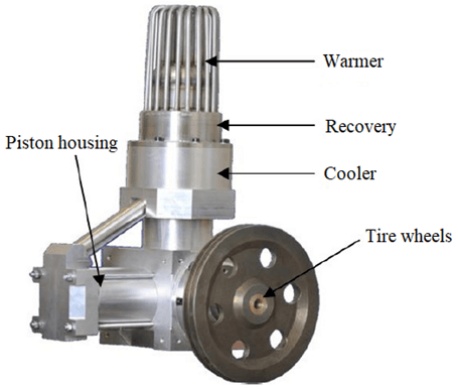

Figure 5 Exterior view of Stirling engine

Table 1 Stirling ST500 engine specifications

Technical characteristics	Values (units)
Output power	500 (watts)
Heat efficiency	8.5%
Standard charge pressure	8 (bar)
Fluid factor	Air, Helium
Frequency of work	14 (Hertz)
Coolant	Water
Movement range of the mandrel	0.75 (Meter)
Movement range of the gas displacer	0.75 (Meter)
Angle mode	90 (degrees)
Type of heater	Tube 20 (× 6 mm)
Cooling type	Tube 144 (× 13 mm square)
Material retrieval	Stainless steel
Heat absorption temperature	350 - 420°C
Heat dissipation temperature	30 - 50°C
Maximum volume	3 - 10 × 1.79) cubic meters
Minimum volume	1.37×10
Compression ratio	1.3: 1

4 Results and discussion

4.1 Test for Stirling refrigerator using air gas

Figure 6 is a schematic of a Gamma Stirling engine for cooling production. Figure 7 shows the power generator connected to a power supply and used for the initial start of the motor. The power generator is also connected to the aircraft wheel using a belt. When the power supply is turned on, the power generator rotates. It rotates and power is transmitted to the flywheel by the belt. In this case, according to the Stirling cycle, the heating part of the device cools down and the temperature has reached below zero degrees after a few short minutes. Copper pipes have been used to measure the amount of heat transfer in the cooling section. To measure the amount of heat transfer, water is first pumped through a copper tube and then the effluent is collected in an insulated chamber. By measuring the outlet water flow from the copper pipes as well as measuring the inlet and outlet water temperature of the copper pipes, the amount of heat transfer in the heating section of the device according to Equation (22) has been obtained [26].

$$\dot{Q} = \dot{m} c_p \Delta T \tag{22}$$

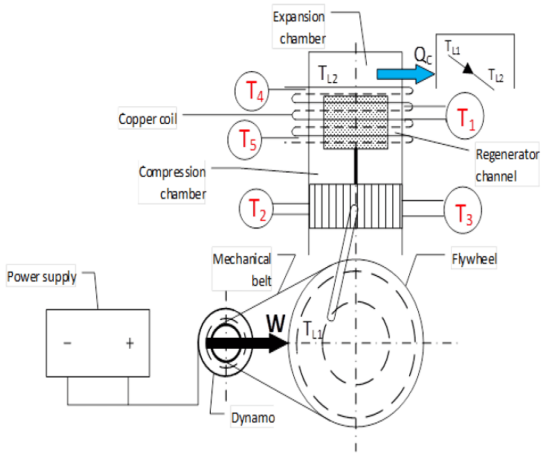

Figure 6 Schematic diagram of Gamma type Stirling refrigerator

Figure 7 Generator to produce power generators

Table 2 and 3 show the initial conditions for the four different tests performed on the Stirling refrigerator to generate cooling using air gas. In these experiments, the air pressure of the operating fluid is 3 times, and the generating power is fixed at 200 and 430.8 watts. Experiments 1, 2, 3 and 4 are performed for 2 to 10 minutes and for all four tests, the discharge flux of the outlet water from the copper pipes is considered constant and equal. For better comparison of the results, the input power is fixed by the power supply.

Table 2 Different laboratory conditions for cooling production

Test	1	2	3	4
Period of source nutrition to be on (minutes)	2	6	8	10
The medium gas pressure	3	3	3	3
Voltage consumption (volts)	20	20	20	20
Electricity Consumption (amps)	10	10	10	10
Power consumption (watts)	200	200	200	200
The initial temperature of cooling section (°C)	14	14	14	14
The final temperature of cooling section (°C)	7.67	-2.52	-5.18	-7.11
Fluid factor	Air	Air	Air	Air

Initially, the Stirling motor is started using a power supply in laboratory conditions at different power, pressure and temperatures. More detailed study and comparison, experiments have

Table 3 Different laboratory conditions for cooling production

Test	1	2	3	4
Period of source nutrition to be on (minutes)	2	6	8	10
The medium of gas pressure (bar)	3	3	3	3
Voltage consumption (volts)	25.8	25.8	25.8	25.8
Electricity consumption (amps)	16.7	16.7	16.7	16.7
Power consumption (watts)	430.8	430.8	430.8	430.8
The initial temperature of cooling section (°C)	17	17	17	17
The final temperature of cooling section (°C)	6.70	-10.29	-15.85	-19.00
Fluid factor	Air	Air	Air	Air

been performed for several times periods in different pressures, power and gases and at each stage, and the cooling temperature has been calculated. The voltage and current of the power supply were equal to 20 volts and 10 amps, respectively, and the ambient temperature in all four experiments was constant and equal to 25°C. According to Figure 6, the temperature of the inlet and outlet parts of the copper pipes at the top and bottom (T4, T5) and the production cooling temperature (T1) have been measured by the temperature reader in Figure 8.

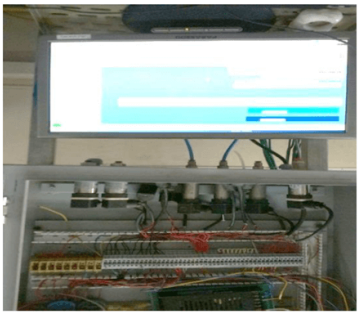

Figure 8 Temperature reader device output with Adam software

The temperature sensor is connected to the temperature reader and using ADAM software (ADAM) has the ability to measure the temperatures of different parts of the test and finally gives us the temperatures at different times in the form of Excel output. The test is performed for several time intervals. At each stage, the internal pressure of the measuring device and the power and experimental efficiency have been calculated. Finally, with the increase of power generator power and fluid gas pressure, the production of refrigerator and cooling work has been witnessed and the temperature of T1 has reached about 7°C. Table 4 shows the initial conditions for the four different tests performed on the Stirling refrigerator to generate cooling using air gas.

Table 4 Different laboratory conditions for cooling production

Test	1	2	3	4
Period of source nutrition to be on (minutes)	10	8	6	2
The medium of gas pressure (bar)	3	3	3	3
Voltage consumption (volts)	31	31	31	31
Electricity consumption (amps)	17	17	17	17
Power consumption (watts)	520.8	520.8	520.8	520.8
The initial temperature of cooling section (°C)	20	20	20	20
The final temperature of cooling section (°C)	-23	-20	-13	5
Fluid factor	Air	Air	Air	Air

In these tests, the air pressure of the operating fluid is 3 times, and the generating power is constantly considered to be 520.8 watts. Experiments 1, 2, 3 and 4 were performed for 2 to 10 minutes. For all four tests, the discharge flux from the copper pipes is considered constant and equal. To better compare the results, the input power by the power supply was constant. The voltage and current of the power supply are equal to 31 volts and 17 amps, respectively, and the ambient temperature in all four experiments is constant and equal to 25 °C. To determine test points and compare values

Heat transfer in the heating section of the Stirling engine, the temperature of the inlet and outlet parts of the copper pipes at the top and bottom (T4, T5) and the production cooling temperature (T1) have been measured by the temperature reader. The gas pressure, the temperature of T1 has reached about 23 °C. In Figure 9 and 10, the cooling output is shown using the ST500 single gamma Stirling motor.

Figure 9 Cooling output by using Gamma Stirling refrigerator

Figure 10 Display of the cooling output gamma Stirling refrigerator

Figure 10 shows the temperature-time diagram for the six experiments performed at pressures of 3 and 6 bar and different powers. As shown, when the power supply is turned on, the temperature of the heating part of the device decreases, and finally, after a certain period of time and increasing the generating power and gas pressure, the temperature of the cooling part of the Stirling engine will be as shown in Figure 11. And the temperature of the cooling part of T1 has reached about -23 degrees Celsius.

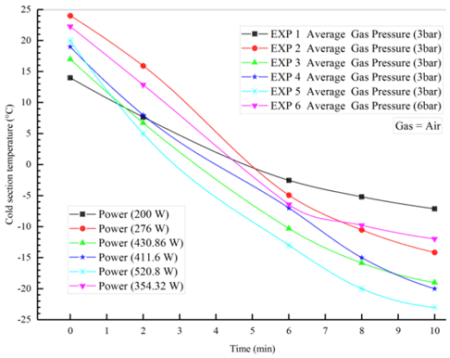

Figure 11 Temperature-time diagram for air gas tests at different pressures for the Stirling engine in cooling mode

4.2 Test for Stirling refrigerator using helium gas

Table 5 shows the initial conditions for four different experiments on the Stirling refrigerator to generate cooling using helium gas.

Table 5 Different laboratory conditions for cooling production

Test	1	2	3	4
Period of source nutrition to be on (minutes)	2	6	8	10
The medium of gas pressure (bar)	3	3	3	3
Voltage consumption (volts)	20	20	20	20
Electricity consumption (amps)	12	12	12	12
Power consumption (watts)	240	240	240	240
The initial temperature of cooling section (°C)	25	25	25	25
The final temperature of cooling section (°C)	10.12	-3.22	-7.77	-9.78
Working fluid	Helium	Helium	Helium	Helium

In these experiments, the pressure of the operating fluid of the air is 3 times and the generating power is constantly considered 240 watts. Experiments 1, 2, 3 and 4 were performed in a period of 2 to 10 minutes. For all four tests, the discharge flux from the copper pipes is considered constant and equal. For better comparison of the results, the input power is fixed by the

power supply. The voltage and current of the power supply are equal to 20 volts and 12 amps, respectively, and the ambient temperature in all four experiments is constant and equal to 25 degrees Celsius. According to Figure 6, the temperature of the inlet and outlet parts of the copper pipes at the top and bottom) T4 and T5 (and the production cooling temperature) T1 (measured by the temperature reader) and finally the temperature of T1 has reached about 10°C. Table 6 shows the initial conditions for the four different tests performed on the Stirling refrigerator to generate cooling using helium gas. In these tests, the air pressure of the operating fluid is 6 times and the generating power is considered to be a constant 420 watts. Experiments 1, 2, 3, and 4 were performed over a period of 2 to 10 minutes. For all four tests, the discharge flux of the outlet water from the copper pipes was considered constant and equal. In order to better compare the results, the input power The voltage and current of the power supply are equal to 20 volts and 21 amps, respectively, and the ambient temperature in all four experiments is constant and equal to 25°C. According to Figure 6, the temperature of the inlet and outlet parts of the pipe. Copper at the top and bottom (T4 and T5) and the production cooling temperature (T1) are measured by the temperature reader, and finally the temperature at T1 has reached about -21°C.

Table 6 Different laboratory conditions for cooling production

Test	1	2	3	4
Period of source nutrition to be on (minutes)	2	6	8	10
The medium of gas pressure (bar)	6	6	6	6
Voltage consumption (volts)	20	20	20	20
Electricity consumption (amps)	21	21	21	21
Power consumption (watts)	420	420	420	420
The initial temperature of cooling section (°C)	15	15	15	15
The final temperature of cooling section (°C)	6.23	-11.74	-17.33	-20.96
Fluid factor	Helium	Helium	Helium	Helium

Also Table 7 shows the comparison of the test results and numerical analysis for helium in the average 5 bar pressure with 300 W Stirling refrigerator power.

Table 7 Comparison between the experiment and numerical simulations

Time (min)	Test temperature (°C)	Numerical temperature (°C)	Error (%)
3	6.25	6.08	2.72
6	-4.43	-4.59	3.61
9	-10.12	-10.27	1.48

Table 8 shows the properties of the operating fluids used at zero Celsius degrees. Less viscous gases will have more output power under similar operating conditions.

Table 8 Sutherland law viscosity variables for gases at 273°K

Type of Gas	Viscosity (N.s/m^2)
Air	1.716 e-5
Argon	2.125 e-5
Nitrogen	1.664 e-5
Hydrogen	8.411 e-6
Helium	1.864 e-4

Katooli et al. [21] experiment was obtained at 3 bar pressure and power of 441.14, 458.5 and 476 watts and was cooled using a gamma Stirling refrigerator and helium operating fluid as can be seen in Figure 12.

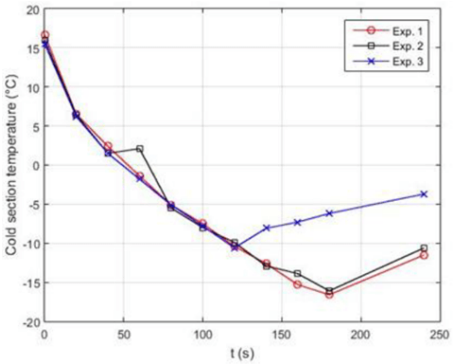

Figure 12 Temperature-time diagram for helium gas experiments [21]

Figure 13 shows the time-temperature diagram for the four performed experiments.

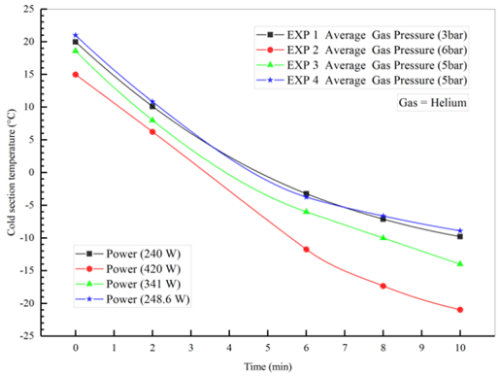

Figure 13 Temperature-time diagram for helium gas experiments at different pressures and Stirling refrigerator mode

As shown, when the power supply is turned on, the temperature of the heater section of the device decreases until the motor of the power supply is switched off. Finally, after a certain period of time, the generator power and gas pressure increase, the cooling temperature section of the Stirling refrigerator will be in the form of Figure 13, and the temperature of the cooling part (T1) will reach about -21 Celsius degrees, which has been validated by the article [17], and with more experiments, more accurate results and graphs have been obtained.

5 Conclusion

In this research, a gamma Stirling motor has been set up to produce cooling using a power supply and using different gases at different powers and pressures. In order to increase the accuracy of ambient temperature and discharge flux, the output water from copper pipes is considered constant and equal, and to better compare the results with the research of others, the input power is also provided by the power supply. With a precise design, selecting and increasing the fluid pressure of the operating system of the Stirling engine and the power consumption of the generator will see a decrease in temperature on the cooling side of the Stirling engine and it will become a refrigerator. Experiments have been performed for several time periods and at each stage, the internal pressure of the measuring device and the power and experimental efficiency have been calculated. Finally, by using a new structure and connecting a gamma-type Stirling engine with a power supply, and by increasing the engine speed and inlet power, the outlet temperature in the cooling part of the engine is reduced. The results of ST-500 Stirling refrigerator tests have been compared with the experimental results of other authorities, which have good compatibility and more accurate results have been obtained.

Heavier gases can also be used in Stirling refrigerators, but these gases are less efficient than lighter gases such as helium and hydrogen due to their properties. Hydrogen gas, due to its stronger heat capacity and less viscosity than helium gas, has higher output power, lower estimation error and higher heat efficiency under similar operating conditions, and air can be used in smaller model engines. Theoretically, the use of a light gas such as hydrogen, air or helium as the operating fluid is recommended due to its low viscosity, strong heat transfer coefficient, poor viscosity coefficient, low leakage potential and lack of oxidizing properties. Although low molecular weight means an increase in the rate of fluid leakage from the engine, resulting in a drop in pressure, reduced efficiency, and increased costs (fluid refilling), the heat temperature of the heat exchanger can cause oxidation and corrosion of the components. It should be noted that one of the most effective factors on efficiency is the temperature of the heat source. In addition, by increasing the input power of the power supply, increasing the initial supply pressure of the motor and selecting the appropriate fluid will increase more cooling output in the heat sink of the Stirling refrigerator.

In this research the experiments with Stirling Gamma engine for generation refrigeration effect is performed. Result shows that air fluid with power of 520.8 W at operating pressure 3 bar in 10 minutes could reach to temperature - 23°C and with Helium fluid using power 420 W at operating pressure 6 bar in 10 minutes could reach to temperature -21°C. During experimental implementation less than 10 percent error is accomplished, resulting from various part of engine like, insulation, leaking, belt lash and measurement devise. The results of this research can be used to produce cooling energy in various industries.

Abbreviations

Distance between the shaft axis and the surface of the shaft, m	a1
Distance between the shaft axis and the displacement surface, m	a2
Displacement height, m	a3
Distance between the crankshaft and the crankshaft axis, m	b1
The distance between the displacement shaft axis and the crankshaft axis is, m	b2
Distance between the crankshaft and the crankshaft axis, m	c1
The distance between the displacement bed and the crankshaft axis is, m	c2
The length of the handle handle, m	l1
Length of gas displacement pump handle, m	l2
The length of the handle handle, m	L
Crankshaft radius, m	rc
Lagrange in variable	Lθ
Number of network inputs	J
Wheel rotational torque, m^2kg	Jc
Inhibition volume length, m	X
Mass of parts with reciprocating motion, kg	m
Angle of inclination, Radian	θ
Crankshaft rotational speed, Radian /s	θ
Crankshaft rotational acceleration, Radian /s^2	θ
Mode of movement of gas and displacement of gas, R	Φ

Author contributions

All authors contributed to the study conception and design. Material preparation, data collection and analysis were performed by Rahim Zahedi. The first draft of the manuscript was written by Sareh Daneshgar and Hamidreza Asemi and all authors commented on previous versions of the manuscript. Rahim Zahedi supervised the manuscript. All authors read and approved the final manuscript.

Competing interests

The authors have no relevant financial or non-financial interests to disclose.

Data availability

Datasets analyzed during the current study are available and can be given following a reasonable request from the corresponding author.

References

[1] Ghodrati A, Zahedi Rand Ahmadi A. Analysis of cold thermal energy storage using phase change materials in freezers. Journal of Energy Storage, 2022, **51**: 104433. https://doi.org/10.1016/j.est.2022.104433

[2] Chen WL, Wong KL and Chen HE. An experimental study on the performance of the moving regenerator for a γ-type twin power piston Stirling engine. Energy conversion and management, 2014, **77**: 118-128. https://doi.org/10.1016/j.enconman.2013.09.030

[3] Zahedi R, Daneshgar S and Golivari S. Simulation and optimization of electricity generation by waste to energy unit in Tehran. Sustainable Energy Technologies and Assessments, 2022, **53**: 102338. https://doi.org/10.1016/j.seta.2022.102338

[4] Gheith R, Hachem H, Aloui F, *et al*. Stirling engines. Comprehensive Energy Systems, 2018, **4**: 169-208. https://doi.org/10.1016/B978-0-12-809597-3.00409-0

[5] Urieli I and Berchowitz DM. Stirling cycle engine analysis. 1984.

[6] Kongtragool B and Wongwises S. A review of solar-powered Stirling engines and low temperature differential Stirling engines. Renewable and Sustainable energy reviews, 2003, **7**(2): 131-154. https://doi.org/10.1016/S1364-0321(02)00053-9

[7] Zahedi R, Eskandarpanah R, Akbari M, *et al*. Development of a New Simulation Model for the Reservoir Hydropower Generation. Water Resour Manage, 2022, **36**: 2241-2256. https://doi.org/10.1007/s11269-022-03138-9

[8] Walker G. Stirling-cycle machines. Oxford, Clarendon Press, 1973.

[9] Kaldehi BJ, Keshavarz A, Pirooz AA, *et al*. Designing a micro Stirling engine for cleaner production of combined cooling heating and power in residential sector of different climates. Journal of Cleaner Production, 2017, **154**: 502-516. https://doi.org/10.1016/j.jclepro.2017.04.006

[10] Prakash S and Guruvayurappan A. Using stirling engine to increase the efficiency of an IC engine. in The World Congress on Engineering 2011, London, UK, 2011.

[11] Hooshang M, Moghadam RA and AlizadehNia S. Dynamic response simulation and experiment for gamma-type Stirling engine. Renewable energy, 2016, **86**: 192-205. https://doi.org/10.1016/j.renene.2015.08.018

[12] Hooshang M, Moghadam RA, Nia SA, *et al*. Optimization of Stirling engine design parameters using neural networks. Renewable Energy, 2015, **74**: 855-866. https://doi.org/10.1016/j.renene.2014.09.012

[13] Zahedi R and Rad AB. Numerical and experimental simulation of gas-liquid two-phase flow in 90-degree elbow. Alexandria Engineering Journal, 2022, **61**(3): 2536-2550. https://doi.org/10.1016/j.aej.2021.07.011

[14] Dai D, Yuan F, Long R, *et al*. Imperfect regeneration analysis of Stirling engine caused by temperature differences in regenerator. Energy Conversion and Management, 2018, **158**: 60-69. https://doi.org/10.1016/j.enconman.2017.12.032

[15] Mahmoodi M. and Ziabasharhagh M. Numerical solution of beta-type Stirling engine by optimizing heat regenerator for increasing output power and efficiency. Journal of Basic Application Science Research, 2012, **2**: 1395-1406.

[16] Erbay LB, Ozturk MM and Doan B. Overall performance of the duplex Stirling refrigerator. Energy Conversion and Management, 2017, **133**: 196-203. https://doi.org/10.1016/j.enconman.2016.12.003

[17] Ansarinasab H and Mehrpooya M. Investigation of a combined molten carbonate fuel cell, gas turbine and stirling engine combined cooling heating and power (CCHP) process by exergy cost sensitivity analysis. Energy conversion and management, 2018, **165**: 291-303. https://doi.org/10.1016/j.enconman.2018.03.067

[18] Damirchi H, Najafi G, Alizadehnia S, *et al*. Micro combined heat and power to provide heat and electrical power using biomass and Gamma-type Stirling engine. Applied Thermal Engineering, 2016, **103**: 1460-1469. https://doi.org/10.1016/j.applthermaleng.2016.04.118

[19] Turkyilmazoglu M. Combustion of a solid fuel material at motion. Energy, 2020, **203**: 117837. https://doi.org/10.1016/j.energy.2020.117837

[20] Turkyilmazoglu M. Cooling of particulate solids and fluid in a moving bed heat exchanger. Journal of Heat Transfer, 2019, **141**(11): 114501. https://doi.org/10.1115/1.4044590

[21] Katooli MH, Moghadam RA and Hajinezhad A. Simulation and experimental evaluation of Stirling refrigerator for converting electrical/mechanical energy to cold energy. Energy conversion and management, 2019, **184**: 83-90. https://doi.org/10.1016/j.enconman.2019.01.014

[22] Amarloo AValian AK, Batooei A, *et al*. Thermodynamic analysis of performance parameter of a novel 3 cylinder Stirling engine configuration. Modares Mechanical Engineering, 2017, **16**(10): 448-458.

[23] Daneshgar S and Zahedi R. Optimization of power and heat dual generation cycle of gas microturbines through economic, energy and environmental analysis by bee algorithm. Energy Reports, 2022, **8**: 1388-1396. https://doi.org/10.1016/j.egyr.2021.12.044

[24] Beni HM and Mortazavi H. Mathematical modeling of the solar regenerative heat exchanger under turbulent oscillating flow: Applications of renewable and sustainable energy and artificial heart. Results in Engineering, 2021, **13**: 100321. https://doi.org/10.1016/j.rineng.2021.100321

[25] Lv C, Chang J, Yu D, *et al*. Multivariable control of regeneratively-cooled scramjet engine with two-stage kerosene injection based on H∞ method. Results in Engineering, 2020, **7**: 100161. https://doi.org/10.1016/j.rineng.2020.100161

[26] Zahedi R and Daneshgar S. Exergy analysis and optimization of Rankine power and ejector refrigeration combined cycle. Energy, 2022, **240**: 122819. https://doi.org/10.1016/j.energy.2021.122819